A THIRD-ORDER-CLOSURE MODEL

FOR THE EVOLUTION
OF A CONVECTIVE PLANETARY BOUNDARY LAYER

BY

J. C. ANDRÉ

ETABLISSEMENT D'ETUDES ET DE RECHERCHES MÉTÉOROLOGIQUES, PARIS

FRANCE

1. High-order-closure models

In a turbulent layer, instantaneous velocity and temperature are rapidly varying functions of position and time. It is then necessary, for practical and theoretical reasons, to average these parameters, that is to consider the equations for the mean parameters. But theories of turbulence constructed by means of these equations give rise to the closure problem. In these equations the advection terms are nonlinear in the second order and consequently the evolution of an ith order correlation will involve (i+1)th order correlations. For example, second order terms such as the Reynolds stresses will appear in the equation for the rate of change of the mean velocity, and the turbulent kinematic heat flux will appear in the equation for the rate of change of the mean temperature. An attempt to derive the equations governing double correlations would lead to the introduction of new unknowns, chiefly third order correlations, and so on. As a result the exact system describing turbulent flows is an infinite hierarchy and it is then necessary to introduce a further hypothesis called a closure assumption..

In the case of vertically inhomogeneous turbulence, which is relevant for planetary boundary layer problems, different kinds of closure assumptions are now available. One usually distinguishes two kinds of closure approximations which lead to different turbulence theories: the semi-empirical approach which is based on phenomenological relations between double correlations and the mean flow, on the one hand; and the high-order-closure approach where the closure assumption is made on higher order correlation terms, on the other hand.

The semi-empirical theories often postulate that the local turbulent flux $\overline{u_i'\alpha'}$ of a parameter α is related to the corresponding mean gradient $\partial\overline{\alpha}/\partial x_i$ in the same way as in viscous flow theory. This proportionality then leads to the introduction of unknown eddy viscosities K_α . Furthermore, a simple physical argument shows that K_α should be generally positive. An important consequence of this assumption is that the vertical heat flux $\overline{w'T'}$ and the temperature gradient $-\partial\overline{T}/\partial z$ always have the same sign. Unfortunately this is not true in convective situations (see e.g. Deardorff, 1966; Turner, 1973). Improved semi-empirical theories like the mixing length approach (Prandtl, 1925) or Smagorinsky's formulation (Smagorinsky, 1963) suffer from the same basic deficiency as shown by Monin and Yaglom (1971).

The high-order-closure method consists in closing the hierarchy of dynamic equations at a higher order. One then has to derive the exact dynamic equations for second (or possibly higher) order correlations and the closure approximation affects only the next higher order correlations. One can consequently

hope that the resulting theory will be more accurate for double correlations and mean values. First examples of such methods are the closure schemes developed by Daly and Harlow (1970), Donaldson (1973), Wyngaard et al. (1974), Lumley and Khajeh-Nouri (1974) and Launder, Reece and Rodi (1975), among others. In these studies the triple correlations are modeled with the use of an ad hoc gradient-diffusion hypothesis or a functional expansion technique. A second example of such methods is the quasi-normal approximation (Millionshchikov, 1941) in which the fourth order correlations are related to second order ones by assuming that velocity is a Gaussian random variable.

An alternative method which partially avoids the use of high-order-closure techniques is the so-called subgrid-scale theory (see e.g. Deardorff, 1972) in which the closure assumption is less crucial since the grid size is then sufficiently small to allow explicit description of most of the turbulent structures. But this requires a three-dimensional simulation, contrary to the preceding approaches, and the memory capacity of the computer restricts considerably the size of the domain which can thus be simulated.

Several models are now available for the description of convective planetary boundary layers (PBL). Clarke (1974) has rewieved the models based on semi-empirical theories and his conclusion is that these models can describe the overall thermal behavior but not many wind characteristics of the PBL. Among the models based on high-order-closure approach, the models of Lewellen and Teske (1973), Wyngaard and Coté (1974) and Yamada and Mellor (1975) simulate fairly well the diurnal course of mean wind and mean temperature but we shall see in the following section that they suffer from another deficiency. Finally the three-dimensional subgrid-scale models of Deardorff (1974a and 1974b) and Soumèria (1976) are the best tools for a precise description of the turbulent PBL but the price to pay for them is very high (it takes about 10 hours of computer time with a CDC 7600 machine to simulate a one hour evolution).

Our purpose is to show what could be a relatively cheap model which could reproduce, with a good agreement, the turbulent structure of the PBL.

2. Second-order-closure models

All the high-order-closure models mentioned in the preceding section could be defined as second-order-closure models. Indeed, they use an equation for the time rate of change of double correlations and the third order correlations which appear in these equations are calculated from additional diagnostic relations.

Triple correlations which appear in second-order-closure models can always be expressed as a sum of terms like $\overline{fu_i'}$ where u_i' is the turbulent fluctuation of the velocity component u_i and f is any product of two turbulent fluctuations. All parametrizations for triple correlations which are presently used in second-order-closure models can be deduced from a simple gradient relation of the form

$$\overline{fu_i'} = - K \, \partial \bar{f} / \partial x_i \qquad (1)$$

where the so-called turbulent diffusivity K is calculated from various second order correlations. For turbulent convection we shall now show that K being a so complicated function of the flow structure, a relation like (1) cannot be used to calculate triple correlations. For this purpose we shall restrict ourselves to the case of the vertical flux $\overline{w'e}$ of turbulent kinetic energy $\bar{e}$

$$\overline{w'e} = \overline{w' \left(u'^2 + v'^2 + w'^2 \right) / 2} \qquad (2)$$

and we shall use for our discussion the results obtained by Willis and Deardorff (1974) in the case of a laboratory experiment concerning penetrative convection, i.e. turbulent convection created by a turbulent heat transfer through a thermally stratified layer of fluid in the absence of mean velocity. In such a case the various proposed parametrizations reduce to:

(i) "single-gradient" expression

$$\overline{w'e} = - K_1 \, \partial \bar{e} / \partial z \qquad (3)$$

where K_1 is given by

either $$K_1 = c_1 \, (\bar{e}/\varepsilon) \, \overline{w'^2} \qquad (4)$$

for Daly and Harlow's (1970) and Wyngaard and Coté's (1974) models (with respectively $c_1 = 0.25$ or $c_1 = 0.3$) where ε is the energy dissipation rate

or $$K_1 = l_1 \, \bar{e}^{\frac{1}{2}} \qquad (5)$$

for Yamada and Mellor's (1975) model where l_1 is a Prandtl's mixing length.

(ii) "double-gradient" expression

$$\overline{w'e} = - K_2 \, \partial(\overline{e}+\overline{w'^2})/\partial z \qquad (6)$$

where K_2 is given by

either $$K_2 = c_2 (\overline{e}/\varepsilon) \overline{w'^2} \qquad (7)$$

for Launder, Reece and Rodi's (1975) model (with $c_2 = 0.11$)

or $$K_2 = l_2 \overline{e}^{\frac{1}{2}} \qquad (8)$$

for Donaldson's (1973) and Lewellen and Teske's (1973) models where l_2 is a mixing length (possibly different from l_1).

Using the experimental values of $\overline{e}$, $\overline{w'^2}$ and ε obtained by Willis and Deardorff (1974), it is possible:

(i) to compute the "theoretical" value of K_1 (resp. K_2) from Eq.(4) (resp. Eq.(7)), to use these values to calculate the "theoretical" kinetic energy flux from Eq.(3) (resp. Eq.(6)) and to compare it to the experimental values of $\overline{w'e}$. This comparison is shown in Fig.1. It can be noticed that single- and double-gradient expressions give almost the same results which do not agree, qualitatively and quantitatively, with experimental values. The qualitative disagreement is crucial since it implies that the divergence of the "theoretical" $\overline{w'e}$ has the wrong sign in most of the upper part of the convective layer. Furthermore, in the lowest part of the convective layer where the divergence has the right sign, its magnitude is too large. These two characteristics show that the upward propagation of turbulence is considerabely underestimated. Finally, the positiveness of $\overline{w'e}$ in the whole convective layer, as compared to the theoretical values of $\overline{w'e}$ calculated with the aid of positive K's, shows that the turbulent diffusivity should be negative at the bottom of the layer (a remark previously made by Wyngaard (1973)) and positive in its upper part (see (ii) for further evidence).

(ii) to compute the two mixing lengths l_1 and l_2 from Eqs.(5) and (8) with the aid of the above calculated "experimental" values of K_1 and K_2 . The results are shown in Fig.2 where we have not represented l_1 for intermediate heights since it has there a very large magnitude (vanishing gradient of kinetic energy). It can be seen that the mixing lengths vary very much with height, therefore reducing their practical usefulness. They are negative in the lower part of the convective layer, and consequently the turbulent diffusivity is also negative, as previously mentioned.

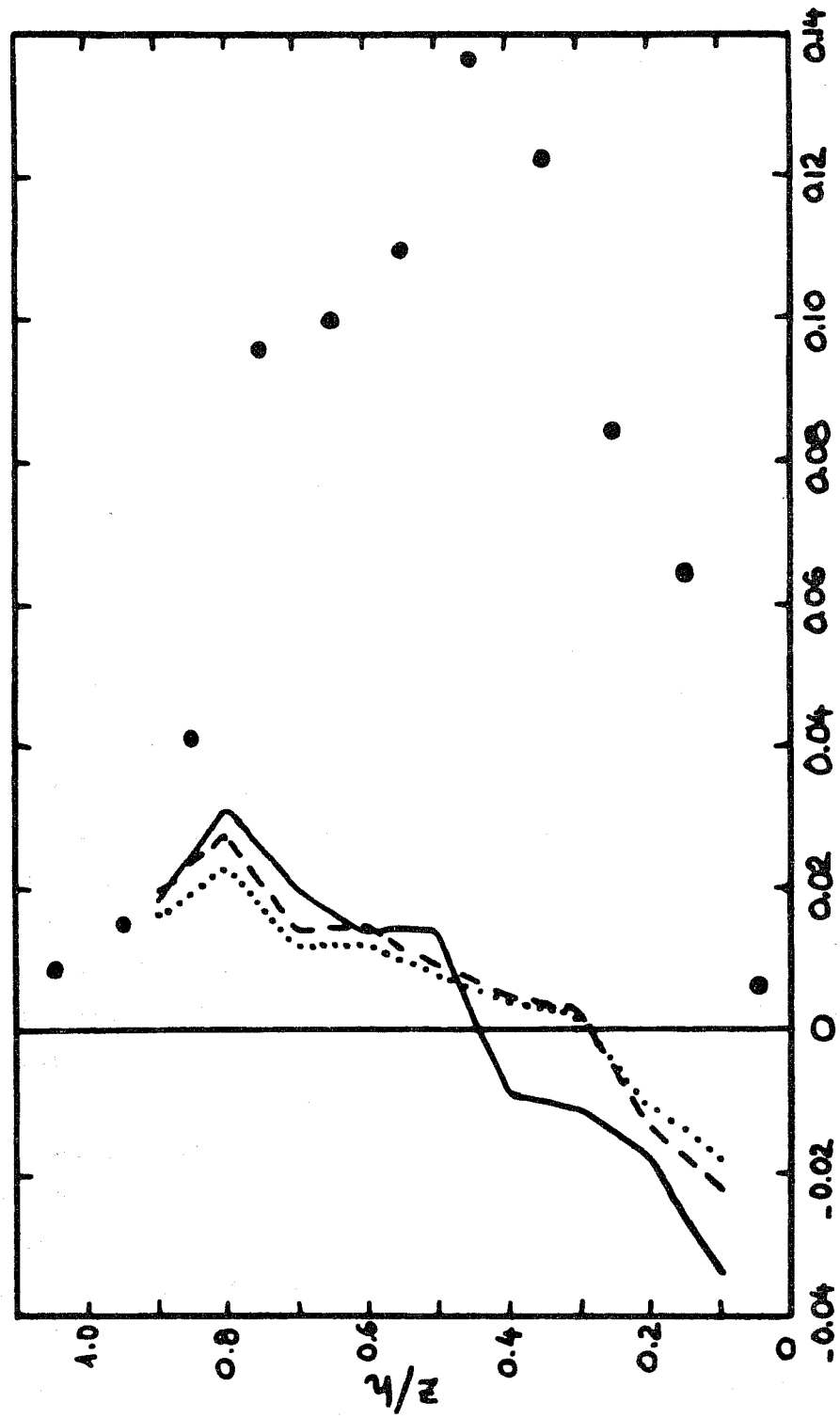

FIGURE 1 - Vertical turbulent flux of eddy kinetic energy as a function of height.
——, Launder, Reece & Rodi (1975); ....., Daly & Harlow (1970); - - -, Wyngaard & Coté (1974);
●, Willis & Deardorff's (1974) measurements.

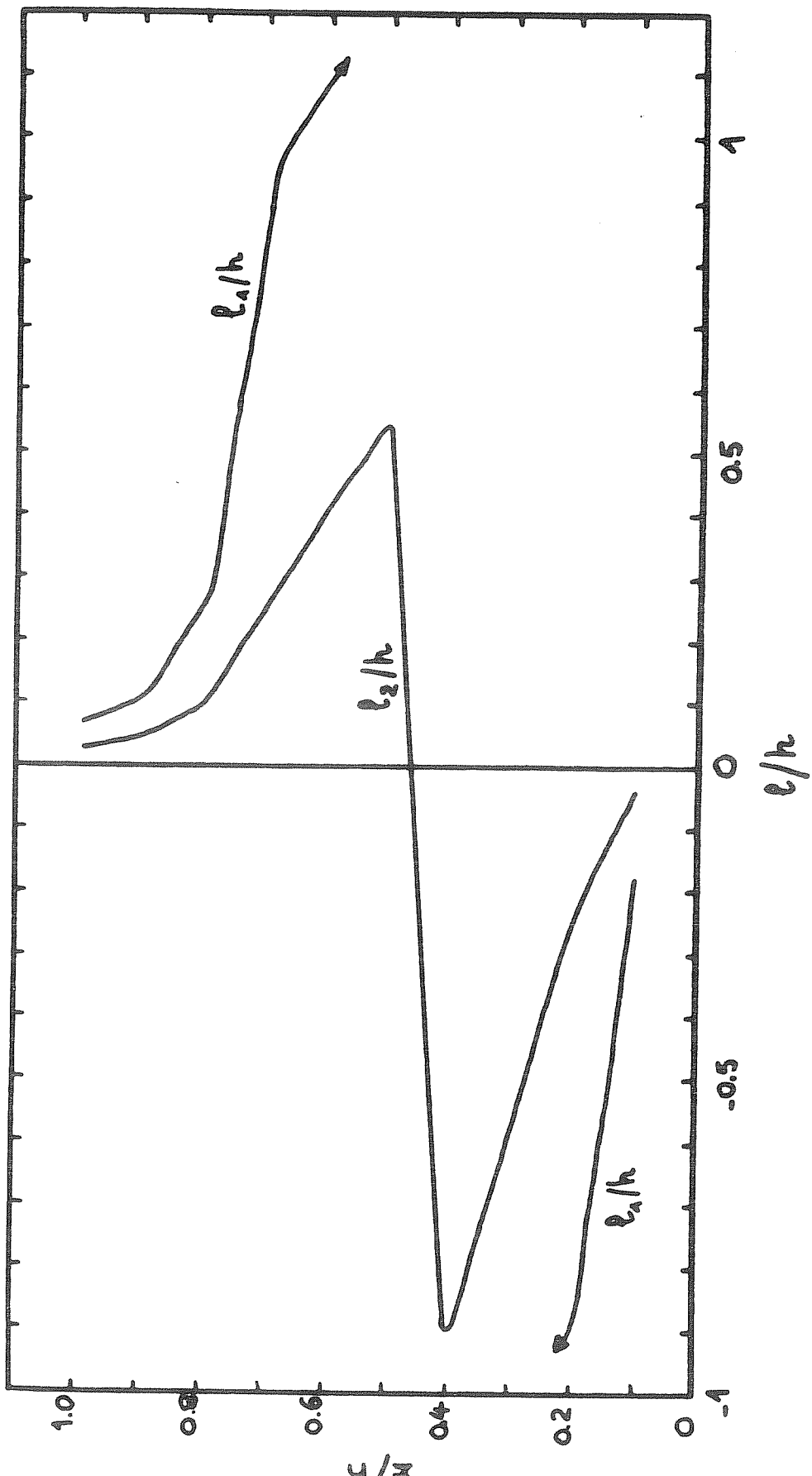

FIGURE 2 - Mixing length as a function of height computed from Willis & Deardorff's (1974) measurements. l_1 is the single-gradient mixing length (Eqs.(3) & (5)); l_2 is the double-gradient mixing length (Eqs.(6) & (8)).

It appears from the above considerations that:

(i) the results issued from double-gradient expression are not notably better than those obtained from single-gradient expression, contrary to the hope of many workers.

(ii) the gradient-relation method is not suitable for the calculation of triple correlations in convective situations and it even perturbs the evolution of double correlations.

It appears then necessary to look for a third-order-closure model if one likes to describe properly the turbulent structure of a convective PBL.

3. A third-order-closure model

* The clipping approximation

A possible third-order-closure model is the quasi-normal model (Millionshchikov, 1941) in which one considers the equations for the rate of change of triple correlations. The equations are closed by assuming that the fourth order correlations are related to the second order ones as in a Gaussian flow. Unfortunately, it was found that the quasi-normal approximation leads to the nonphysical development of negative energy (O'Brien and Francis, 1962; Ogura, 1963). This deficiency of the quasi-normal model can be traced to an excessive growth of triple correlations (Orszag, 1970) since one effect of exact fourth order correlations is to limit the build-up of triple correlations. This effect is obviously lost in the quasi-normal approximation and consequently too large triple correlations can transport energy at a rate larger than the production rate, therefore creating negative energy. One has then to introduce an ad hoc damping mechanism in the equation for the rate of change of triple correlations.

We shall introduce the clipping approximation (André et al., 1976a) which is an example of such a damping mechanism. It is based on the fact that triple correlations between fluctuations of turbulent quantities must verify realizability conditions derived from generalized Schwarz' inequality (Blanchet, 1970; du Vachat, 1976). Given the fluctuations of three turbulent quantities α', β' and γ', the triple correlation $\overline{\alpha'\beta'\gamma'}$ can be expressed as

$$\overline{\alpha'\beta'\gamma'} = \overline{\alpha' \left(\beta'\gamma' - \overline{\beta'\gamma'} \right)} \quad . \tag{9}$$

Now applying Schwarz' inequality to the right-hand side of Eq.(9) we have

$$\overline{\alpha'\beta'\gamma'}^2 \leqslant \overline{\alpha'^2} \left(\overline{\beta'^2\gamma'^2} - \overline{\beta'\gamma'}^2 \right) \quad . \tag{10}$$

If we now use the quasi-normal approximation

$$\overline{\beta'^2\gamma'^2} = \overline{\beta'^2}.\overline{\gamma'^2} + 2\,\overline{\beta'\gamma'}^2 \qquad (11)$$

condition (10) for the realizability of the triple correlation reads, by symmetry

$$\left|\overline{\alpha'\beta'\gamma'}\right| \leqslant \min \left\{ \begin{array}{l} \left[\overline{\alpha'^2}\left(\overline{\beta'^2}.\overline{\gamma'^2} + \overline{\beta'\gamma'}^2\right)\right]^{\frac{1}{2}} \\ \left[\overline{\beta'^2}\left(\overline{\alpha'^2}.\overline{\gamma'^2} + \overline{\alpha'\gamma'}^2\right)\right]^{\frac{1}{2}} \\ \left[\overline{\gamma'^2}\left(\overline{\alpha'^2}.\overline{\beta'^2} + \overline{\alpha'\beta'}^2\right)\right]^{\frac{1}{2}} \end{array} \right\} \qquad (12)$$

But now, nothing in the quasi-normal approximation makes it necessary that this inequality be satisfied. The clipping approximation consists in enforcing inequality (12) at each time step and at each grid point by cutting off the value of the triple correlation $\overline{\alpha'\beta'\gamma'}$ whenever it exceeds the limit imposed by the realizability condition. This indeed constitutes a damping effect of triple correlations. The principal advantage of the quasi-normal theory modified by the clipping approximation is that it produces realizable turbulent flows in the sense that the nonphysical development of negative energy is made impossible, as will be shown numerically.

* The equations for a turbulent PBL

Application of the clipping approximation to Boussinesq turbulence is extensively described in André et al. (1976a). We shall just recall here that, with the aid of Launder's (1975) parametrization for pressure effects and Kolmogorov's arguments for dissipative terms, the equations for mean parameters and double correlations read with usual notations (in the case of horizontally homogeneous flows under the action of gravity g and Coriolis force f):

$$\frac{\partial \overline{u_i}}{\partial t} = -\frac{\partial \overline{u_i'w'}}{\partial z} - \frac{1}{\rho_0}\frac{\partial \overline{p}}{\partial x_i} - f\,\varepsilon_{i3j}\,\overline{u_j} \qquad (13)$$

$$\frac{\partial \overline{\theta}}{\partial t} = -\frac{\partial \overline{w'\theta'}}{\partial z} \qquad (14)$$

$$\frac{\partial \overline{u_i'u_j'}}{\partial t} = -\frac{\partial \overline{u_i'u_j'w'}}{\partial z} - (1-c_5)\left\{\overline{u_i'w'}\frac{\partial \overline{u_j}}{\partial z} + \overline{u_j'w'}\frac{\partial \overline{u_i}}{\partial z} - \alpha g\left(\overline{u_i'\theta'}\,\delta_{3j} + \overline{u_j'\theta'}\,\delta_{3i}\right)\right\} \qquad (15)$$

$$- c_4\frac{\varepsilon}{e}\left(\overline{u_i'u_j'} - \frac{2}{3}\delta_{ij}\,\overline{e}\right) - \frac{2}{3}c_5\,\delta_{ij}\left(\overline{u_k'w'}\frac{\partial \overline{u_k}}{\partial z} - \alpha g\,\overline{w'\theta'}\right) - \frac{2}{3}\delta_{ij}\,\varepsilon$$

$$\frac{\partial \overline{u_i'\theta'}}{\partial t} = -\frac{\partial \overline{u_i'w'\theta'}}{\partial z} - \overline{u_i'w'}\frac{\partial \bar{\theta}}{\partial z} - (1-c_7)\left(\overline{w'\theta'}\frac{\partial \bar{u}_i}{\partial z} - \alpha g\,\overline{\theta'^2}\,\delta_{3i}\right) - c_6\frac{\varepsilon}{e}\overline{u_i'\theta'} \tag{16}$$

$$\frac{\partial \overline{\theta'^2}}{\partial t} = -\frac{\partial \overline{w'\theta'^2}}{\partial z} - 2\,\overline{w'\theta'}\frac{\partial \bar{\theta}}{\partial z} - c_2\frac{\varepsilon}{e}\overline{\theta'^2} \tag{17}$$

where the Coriolis effect on double correlations has been neglected. ε is the kinetic energy dissipation rate given by

$$\varepsilon = c_1\frac{e^{3/2}}{l} \tag{18}$$

where l is the length of energy containing eddies, that is the height of the turbulent layer.

The system governing the evolution of triple correlations can be deduced with a little algebra. In this system appear:
(i) fourth order correlations which will be expressed with the aid of quasi-normal relations (11);
(ii) terms expressing the action of molecular diffusion which, in the absence of sufficient knowledge of their effects, will be neglected;
(iii) terms arising from Coriolis effect which are known to be negligeable (Deardorff, 1974a) and which will be set equal to zero;
(iv) terms expressing pressure effects. These terms will be calculated using a generalization of return-to-isotropy concept:

$$\overline{p'\left(\frac{\partial u_i'u_j'}{\partial z} + \frac{\partial u_i'w'}{\partial x_j} + \frac{\partial u_j'w'}{\partial x_i}\right)} = -c_8\frac{\varepsilon}{e}\overline{u_i'u_j'w'}$$

$$\overline{p'\left(\frac{\partial u_j'\theta'}{\partial x_i} + \frac{\partial u_i'\theta'}{\partial x_j}\right)} = \overline{p'\left(\frac{\partial u_j'\theta'}{\partial x_i} + \frac{\partial u_i'\theta'}{\partial x_j} - \frac{2}{3}\delta_{ij}\frac{\partial u_k'\theta'}{\partial x_k}\right)} + \frac{2}{3}\delta_{ij}\,\overline{p'\frac{\partial u_k'\theta'}{\partial x_k}}$$

$$= -c_8\frac{\varepsilon}{e}\left(\overline{u_i'u_j'\theta'} - \frac{1}{3}\delta_{ij}\,\overline{u_k'u_k'\theta'}\right) - c_9\frac{\varepsilon}{e}\delta_{ij}\,\overline{u_k'u_k'\theta'}$$

$$\overline{p'\frac{\partial \theta'^2}{\partial x_i}} = -c_8\frac{\varepsilon}{e}\overline{u_i'\theta'^2} \quad ; \tag{19}$$

(v) realizability conditions obtained by specialization of inequality (12).

The system reads finally:

$$\frac{\partial \overline{u_i'u_j'w'}}{\partial t} = -\overline{u_i'w'^2}\frac{\partial \overline{u_j}}{\partial z} - \overline{u_j'w'^2}\frac{\partial \overline{u_i}}{\partial z} - \overline{w'^2}\frac{\partial \overline{u_i'u_j'}}{\partial z} - \overline{u_j'w'}\frac{\partial \overline{u_i'w'}}{\partial z} - \overline{u_i'w'}\frac{\partial \overline{u_j'w'}}{\partial z}$$

$$+\alpha g\left(\overline{u_i'u_j'\theta'} + \overline{u_i'w'\theta'}\,\delta_{3j} + \overline{u_j'w'\theta'}\,\delta_{3i}\right) - c_8\frac{\varepsilon}{\underline{\underline{e}}}\overline{u_i'u_j'w'}$$

$$\left|\overline{u_i'u_j'w'}\right| \leqslant \min\left\{\left[\overline{u_i'^2(u_j'^2.w'^2+u_j'w'^2)}\right]^{\frac{1}{2}}, \left[\overline{u_j'^2(u_i'^2.w'^2+u_i'w'^2)}\right]^{\frac{1}{2}}, \left[\overline{w'^2(u_i'^2.u_j'^2+u_i'u_j'^2)}\right]^{\frac{1}{2}}\right\} \quad (20)$$

$$\frac{\partial \overline{u_i'u_j'\theta'}}{\partial t} = -\overline{u_i'u_j'w'}\frac{\partial \overline{\theta}}{\partial z} - \overline{u_i'w'\theta'}\frac{\partial \overline{u_j}}{\partial z} - \overline{u_j'w'\theta'}\frac{\partial \overline{u_i}}{\partial z} - \overline{w'\theta'}\frac{\partial \overline{u_i'u_j'}}{\partial z} - \overline{u_i'w'}\frac{\partial \overline{u_j'\theta'}}{\partial z}$$

$$-\overline{u_j'w'}\frac{\partial \overline{u_i'\theta'}}{\partial z} + \alpha g\left(\overline{u_i'\theta'^2}\,\delta_{3j} + \overline{u_j'\theta'^2}\,\delta_{3i}\right) - c_8\frac{\varepsilon}{\underline{\underline{e}}}\overline{u_i'u_j'\theta'}$$

$$+\left(\frac{1}{3}c_8 - c_9\right)\frac{\varepsilon}{\underline{\underline{e}}}\delta_{ij}\,\overline{u_k'u_k'\theta'}$$

$$\left|\overline{u_i'u_j'\theta'}\right| \leqslant \min\left\{\left[\overline{u_i'^2(u_j'^2.\theta'^2+u_j'\theta'^2)}\right]^{\frac{1}{2}}, \left[\overline{u_j'^2(u_i'^2.\theta'^2+u_i'\theta'^2)}\right]^{\frac{1}{2}}, \left[\overline{\theta'^2(u_i'^2.u_j'^2+u_i'u_j'^2)}\right]^{\frac{1}{2}}\right\} \quad (21)$$

$$\frac{\partial \overline{u_i'\theta'^2}}{\partial t} = -\overline{w'\theta'^2}\frac{\partial \overline{u_i}}{\partial z} - 2\,\overline{u_i'w'\theta'}\frac{\partial \overline{\theta}}{\partial z} - \overline{u_i'w'}\frac{\partial \overline{\theta'^2}}{\partial z} - 2\,\overline{w'\theta'}\frac{\partial \overline{u_i'\theta'}}{\partial z}$$

$$+\alpha g\,\overline{\theta'^3}\,\delta_{3i} - c_8\frac{\varepsilon}{\underline{\underline{e}}}\overline{u_i'\theta'^2}$$

$$\left|\overline{u_i'\theta'^2}\right| \leqslant \left[\overline{\theta'^2(u_i'^2.\theta'^2+u_i'\theta'^2)}\right]^{\frac{1}{2}} \quad (22)$$

$$\frac{\partial \overline{\theta'^3}}{\partial t} = -3\,\overline{w'\theta'^2}\,\frac{\partial \bar{\theta}}{\partial z} - 3\,\overline{w'\theta'}\,\frac{\partial \overline{\theta'^2}}{\partial z}$$

$$\left| \overline{\theta'^3} \right| \leq \left(2\,\overline{\theta'^2}^3 \right)^{\frac{1}{2}} \qquad (23)$$

The values of the constants c_1 to c_9 which are involved in Eqs.(15) to (22) are given by

$$c_1 = 1.6 \;;\; c_2 = 2.5 \;;\; c_4 = 4.5 \;;\; c_5 = 0. \;;$$
$$c_6 = 4.85 \;;\; c_7 = 0.394 \;;\; c_8 = 8. \;;\; c_9 = c_8/3 \;. \qquad (24)$$

* Numerical schemes and boundary conditions

They are described with some details in André et al. (1976b). We shall just say that we use a staggered grid and the Euler-backward time integration scheme and that boundary conditions for double correlations are expressed with the aid of Monin and Obukhov's (1954) similarity theory.

* Accuracy of triple correlations modelling

When applied to the Willis and Deardorff's penetrative convection experiment ($\overline{u_i} = 0$), the model reduces to a set of 11 prognostic equations and 6 realizability inequalities (André et al., 1976b). In such a case the numerical profile of $\overline{w'e} = \frac{1}{2}\,\overline{w'u_k'u_k'}$ is shown in Fig. 3. The particularly good agreement between computed and experimental curves justifies the validity and accuracy of the clipping approximation. Indeed it gives the right values of the vertical flux of eddy kinetic energy, a physically important triple correlation.

It is interesting to look at the overall frequency of enforcement of realizability inequalities. This frequency is 0 % for $\overline{w'^3}$, 11 % for $\overline{w'^2\theta'}$, 6 % for $\overline{w'\theta'^2}$, 85 % for $\overline{\theta'^3}$, 0 % for $\overline{u'^2w'}$ and $\overline{u'^2\theta'}$. It is not surprising that $\overline{\theta'^3}$ has to be frequently controlled since it is the only parameter for which pressure fluctuations do not damp the evolution. We shall finally indicate that if realizability conditions are not enforced, i.e. if one uses the quasi-normal approximation alone, some triple correlations develop rapidly very large values, therefore inducing a blow-up of the quasi-normal model.

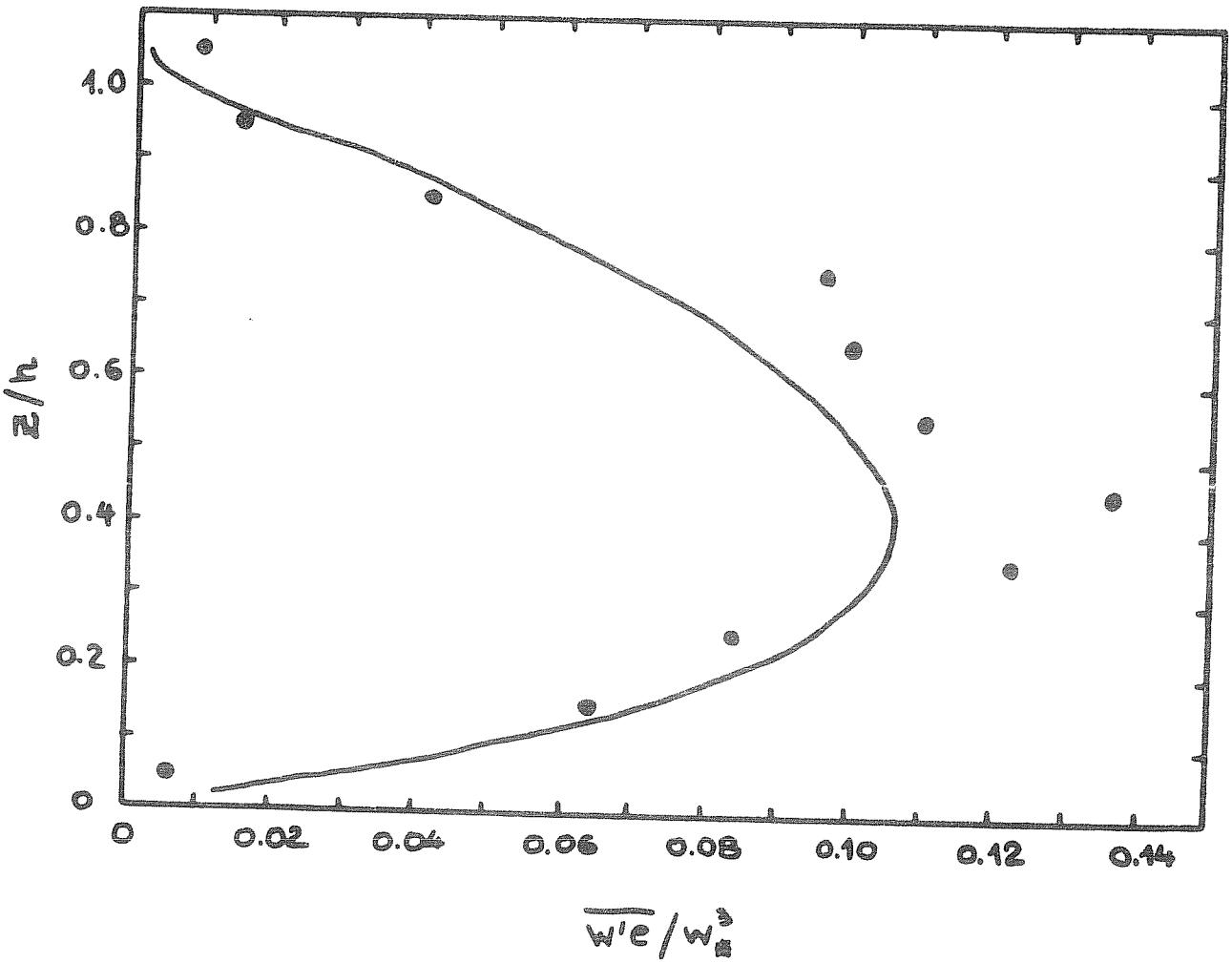

FIGURE 3 - Vertical turbulent flux of eddy kinetic energy as a function of height. _____, model results; ●, Willis & Deardorff's (1974) measurements.

4. Comparison with the Wangara data

The above presented and discussed clipping approximation will be now applied to the description of the well-known Day 33 of the Wangara experiment (Clarke et al., 1971). In this case the system (13)-(23) governs:

(i) 3 mean quantities: $\overline{u}$, $\overline{v}$ and $\overline{\theta}$ (Eqs.(13) and (14));

(ii) 9 double correlations: $\overline{u'^2}$, $\overline{u'w'}$, $\overline{v'^2}$, $\overline{v'w'}$ and $\overline{w'^2}$ (Eq.(15)), $\overline{u'\theta'}$, $\overline{v'\theta'}$ and $\overline{w'\theta'}$ (Eq.(16)) and $\overline{\theta'^2}$ (Eq.(17));

(iii) 14 triple correlations: $\overline{u'^2w'}$, $\overline{u'w'^2}$, $\overline{v'^2w'}$, $\overline{v'w'^2}$ and $\overline{w'^3}$ (Equation and inequality (20)), $\overline{u'^2\theta'}$, $\overline{u'w'\theta'}$, $\overline{v'^2\theta'}$, $\overline{v'w'\theta'}$ and $\overline{w'^2\theta'}$ (Equation and inequality (21)), $\overline{u'\theta'^2}$, $\overline{v'\theta'^2}$ and $\overline{w'\theta'^2}$ (Equation and inequality (22)) and $\overline{\theta'^3}$ (Equation and inequality (23)).

Boundary conditions for the 9 double correlations at their first level are expressed in terms of the kinematic heat flux at ground $Q_o(t)$, of the friction velocity u_* and of the convective velocity $w_* = (\alpha g Q_o h)^{1/3}$, according to the modified surface layer similarity theory for convective situations (see e.g. Wyngaard and Coté, 1974), i.e. (in surface layer axes):

$$\overline{u'^2} = 4\,u_*^2 + 0.2\,w_*^2 \quad ; \quad \overline{v'^2} = 1.75\,u_*^2 + 0.2\,w_*^2 \quad ; \quad \overline{u'v'} = 0$$

$$\overline{w'^2}(z) = \left[1.75 + 2(-z/L)^{2/3}\right] u_*^2 \quad ; \quad \overline{u'w'} = -u_*^2 \quad ; \quad \overline{v'w'} = 0 \qquad (25)$$

$$\overline{w'\theta'} = Q_o \quad ; \quad \overline{u'\theta'}(z) = -3.7\,(1 - 15z/L)^{-1/4}\,(1 - 9z/L)^{-\frac{1}{2}}\,Q_o$$

$$\overline{v'\theta'} = 0 \quad ; \quad \overline{\theta'^2}(z) = 4\,(1 - 8.3z/L)^{-2/3}\,Q_o^2/u_*^2$$

where L is the Monin-Obukhov length ($L = -u_*^3/k\alpha g Q_o$; k = Von Karman constant = 0.35). $Q_o(t)$ is given in order to reproduce as exactly as possible the observed surface temperature evolution

$$Q_o(t) = 0.18 \sin(\pi(t-7.5)/10) \text{ m sec}^{-1} \text{ K} \quad (t \text{ in hours})$$

since u_* is computed with the aid of the Paulson's (1970) formula from the wind velocity at its first level and from a roughness-length which was taken to be 1 cm ; $h = h(t)$, which appears in w_* and also in Eq.(18), is computed from the actual mean temperature profile.

Initial conditions for $\bar{u}$, $\bar{v}$ and $\bar{\theta}$ are taken according to the corresponding experimental profiles at $t = 9$ h , since the other 23 correlations are intially set equal to zero (the numerical model will need approximatively one hour to establish realistic profiles for these correlations). The pressure gradient is taken according to the estimated geostrophic wind (Wyngaard and Coté, 1974):

$$u_G\ (\text{msec}^{-1}) = \begin{cases} -5.5 + 2.9\ 10^{-3}\ z & \text{for } z \leqslant 1000 \text{ m} \\ -2.6 + 1.4\ 10^{-3}\ z & \text{for } 1000 \text{ m} \leqslant z \leqslant 2000 \text{ m} \end{cases}$$

$$v_G = 0 \qquad . \qquad (26)$$

The simulation is stopped at $t = 17^{\text{h}}\ 30$ when the prescribed surface heat flux Q_o vanishes.

We used a 40-level numerical model with a grid size Δz equal to 50 m , the time step Δt being equal to 4 sec .

* Mean parameters results

In Fig. 4 the computed temperature profiles are compared to the measured ones. The agreement is very good, qualitatively and quantitatively, in the adiabatic layer as well as in the unstable surface layer. The "overshoot" region, i.e. the upper part of the convective layer where rising air overshoots its equilibrium height and produces then a cooling of the overlying stable layer, is also recovered and the height of the convective layer as well as the lapse rate around the inversion level are in rather good agreement with experiment. This is an indirect verification of the validity of the clipping approximation since it is known that the erosion of the overlying stable layer depends strongly on the treatment of turbulent fluxes (Deardorff, 1973; Sommeria, 1974).

Figs. 5a to 5d show the evolution of the mean wind during the convective regime. The initial mean wind profile is chosen from the measured wind profile at $t = 9$ h by smoothing out small vertical scale irregularities (Fig. 5a). The evolution is governed by two distinct phenomena:
(i) an intense mixing of momentum in the adiabatic layer due to thermally generated turbulence. This can be seen if one considers the height of the constant wind layer which evolves from 1000 m at $t = 12$ h (Fig. 5b) to 1200 m at $t = 14$ h (Fig. 5c) and 1300 m at $t = 16$ h (Fig. 5d). These heights correspond in fact to the convective layer thickness (see Fig. 4).

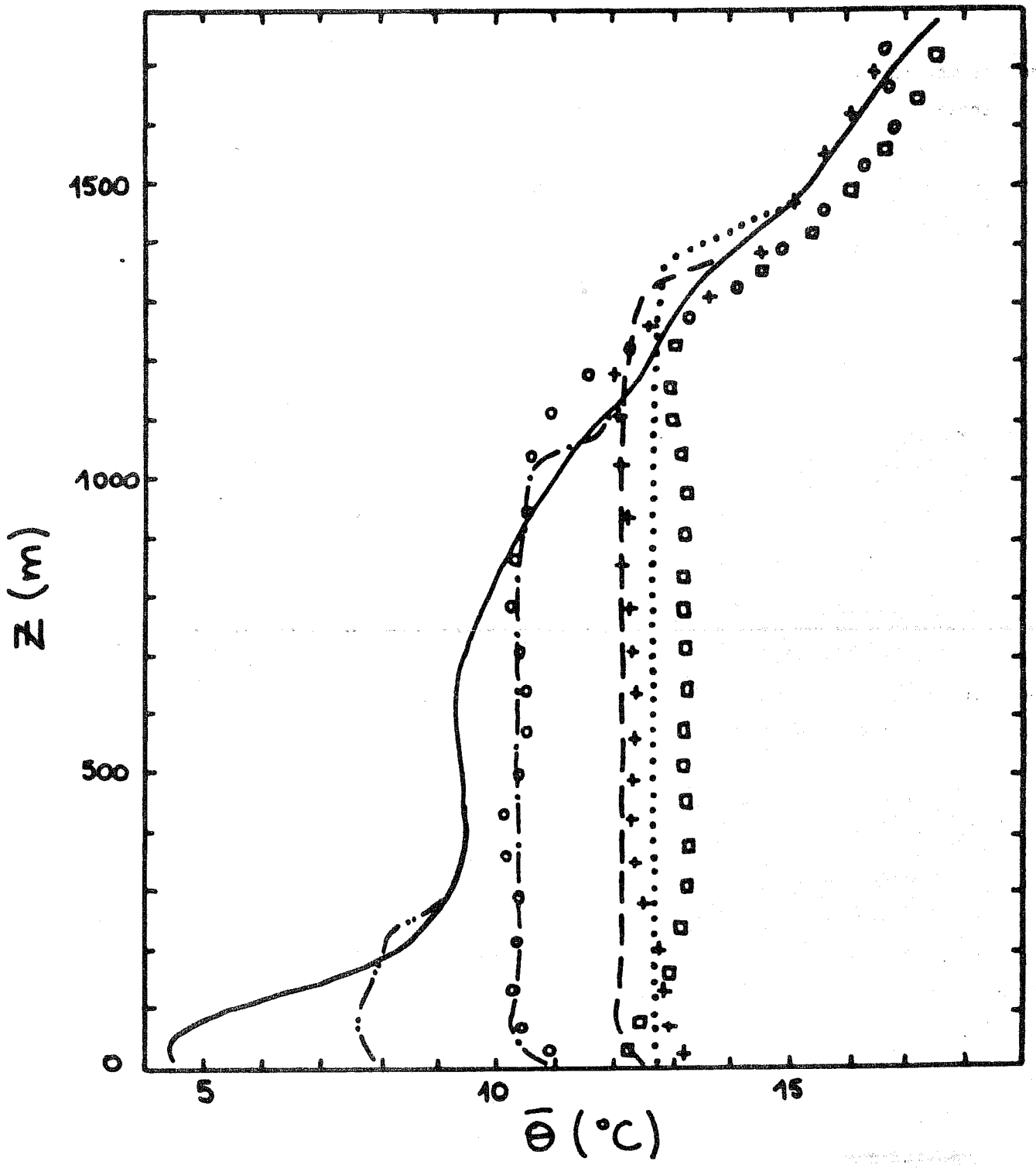

FIGURE 4 - Evolution of the mean temperature profile. 09 h: _____, experimental values and initial condition of the model; 12 h: o, experimental values and -.-.-, numerical profile; 15 h: +, experimental values and - - -, numerical profile; ◘, experimental values at 18 h and ....., numerical profile at 17 h 30.

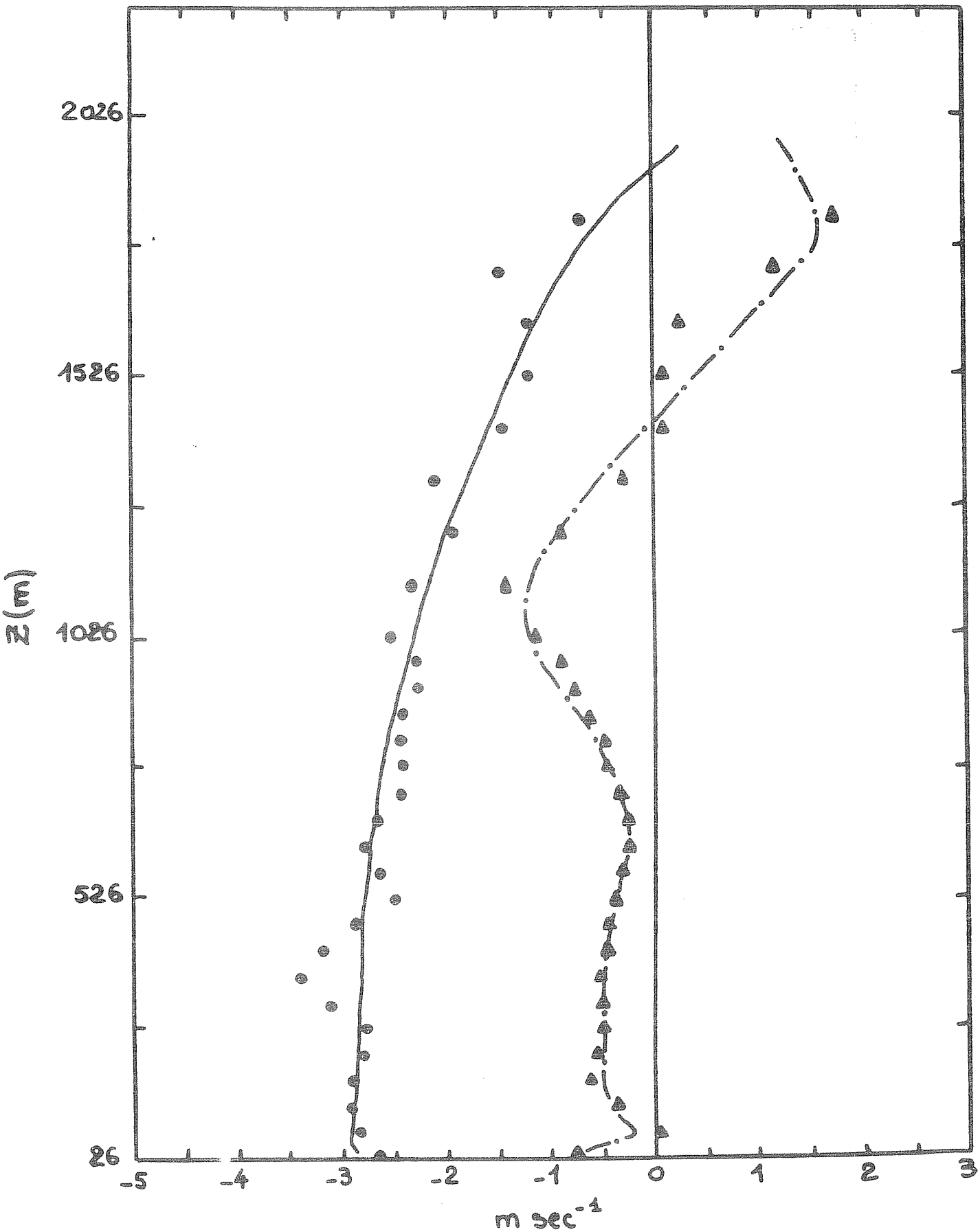

FIGURE 5a - Mean wind profile at 09 h. ●, experimental zonal wind and ____, initial condition of the model; ▲, experimental meridional wind and -.-.-, initial condition of the model.

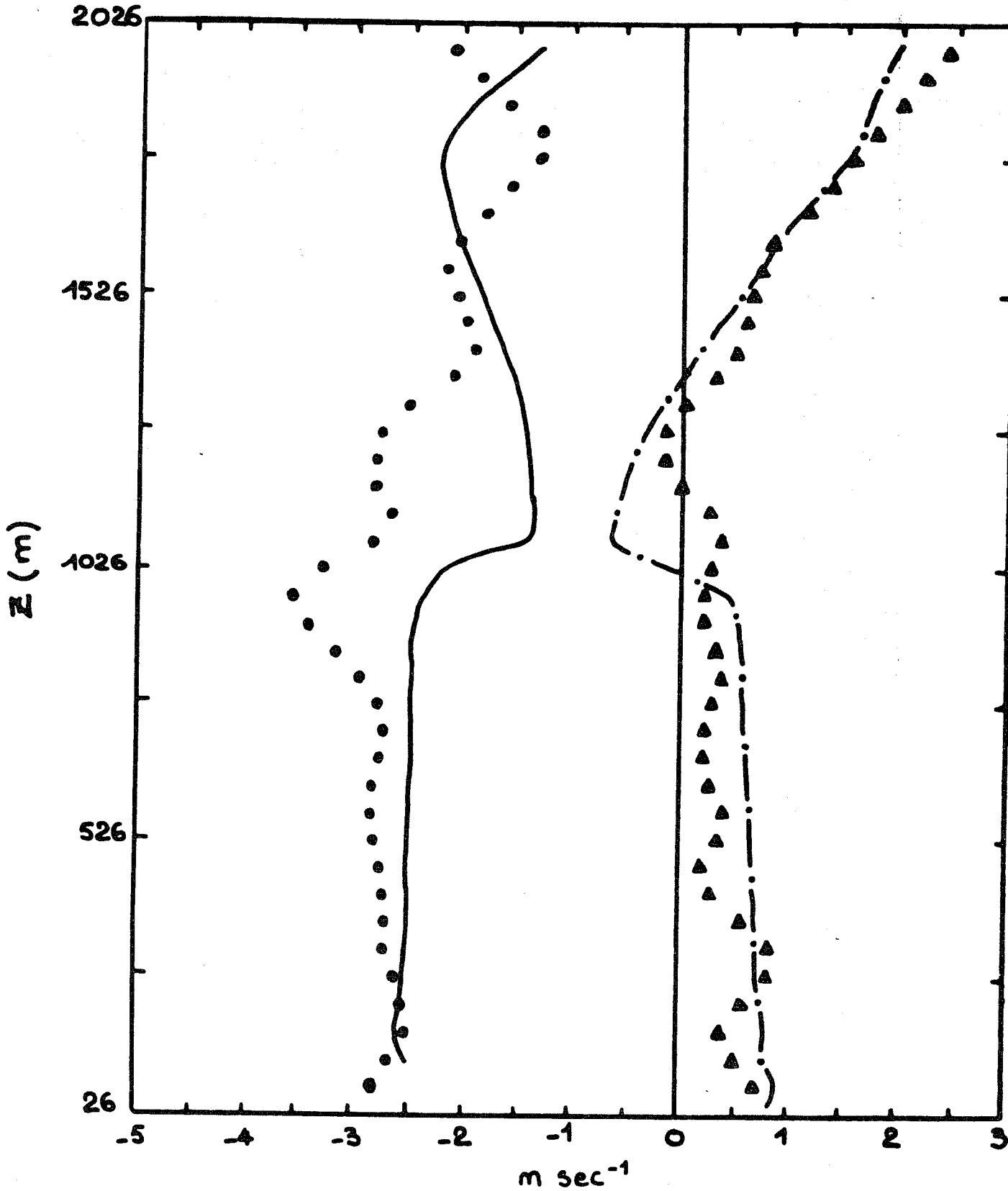

FIGURE 5b - Mean wind profile at 12 h. ●, experimental values and _____, numerical values of the zonal wind; ▲, experimental values and -.-.-, numerical values of the meridional wind.

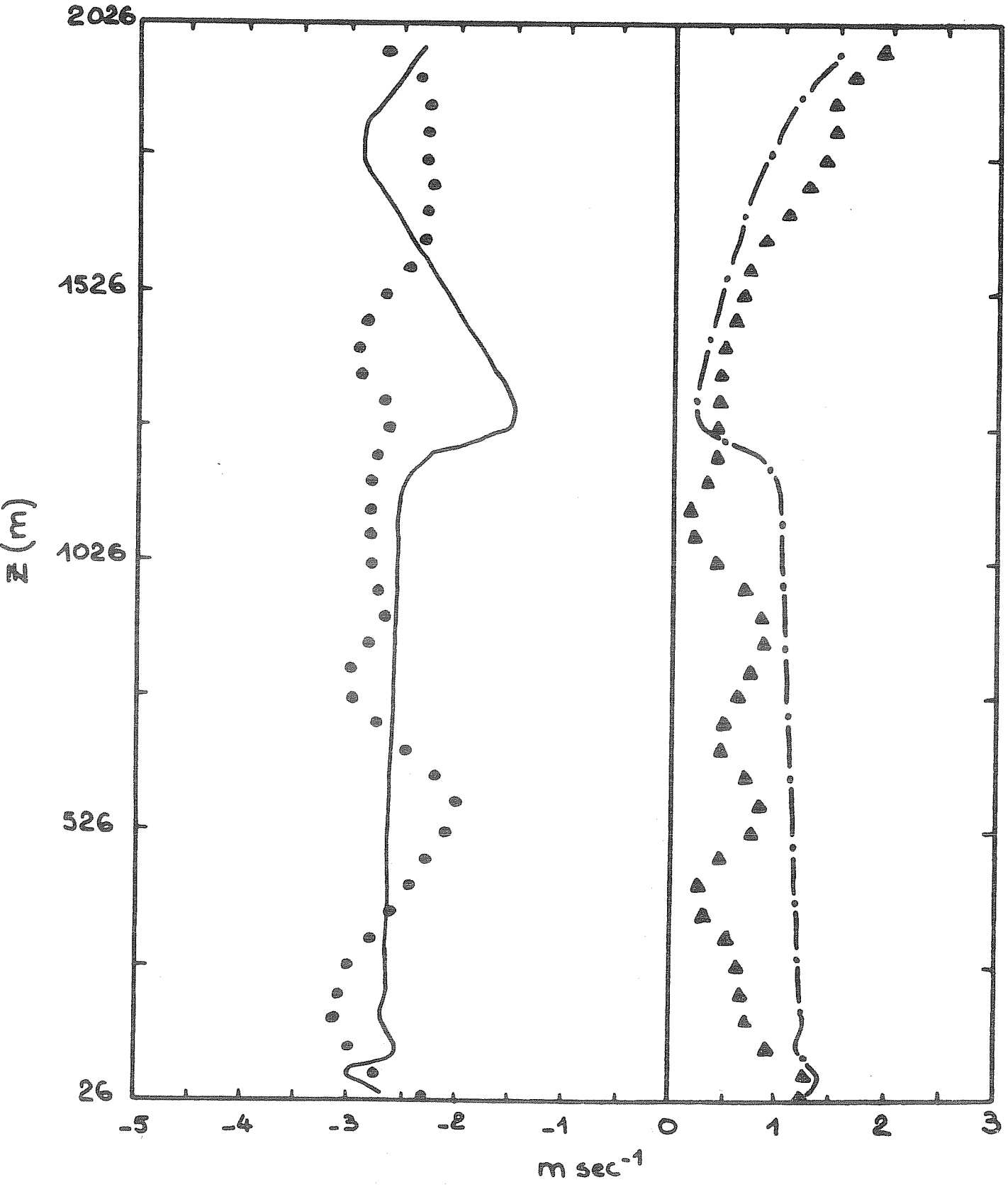

FIGURE 5c - Mean wind profile at 14 h. ●, experimental values and _____, numerical values of the zonal wind; ▲, experimental values and -.-.-, numerical values of the meridional wind.

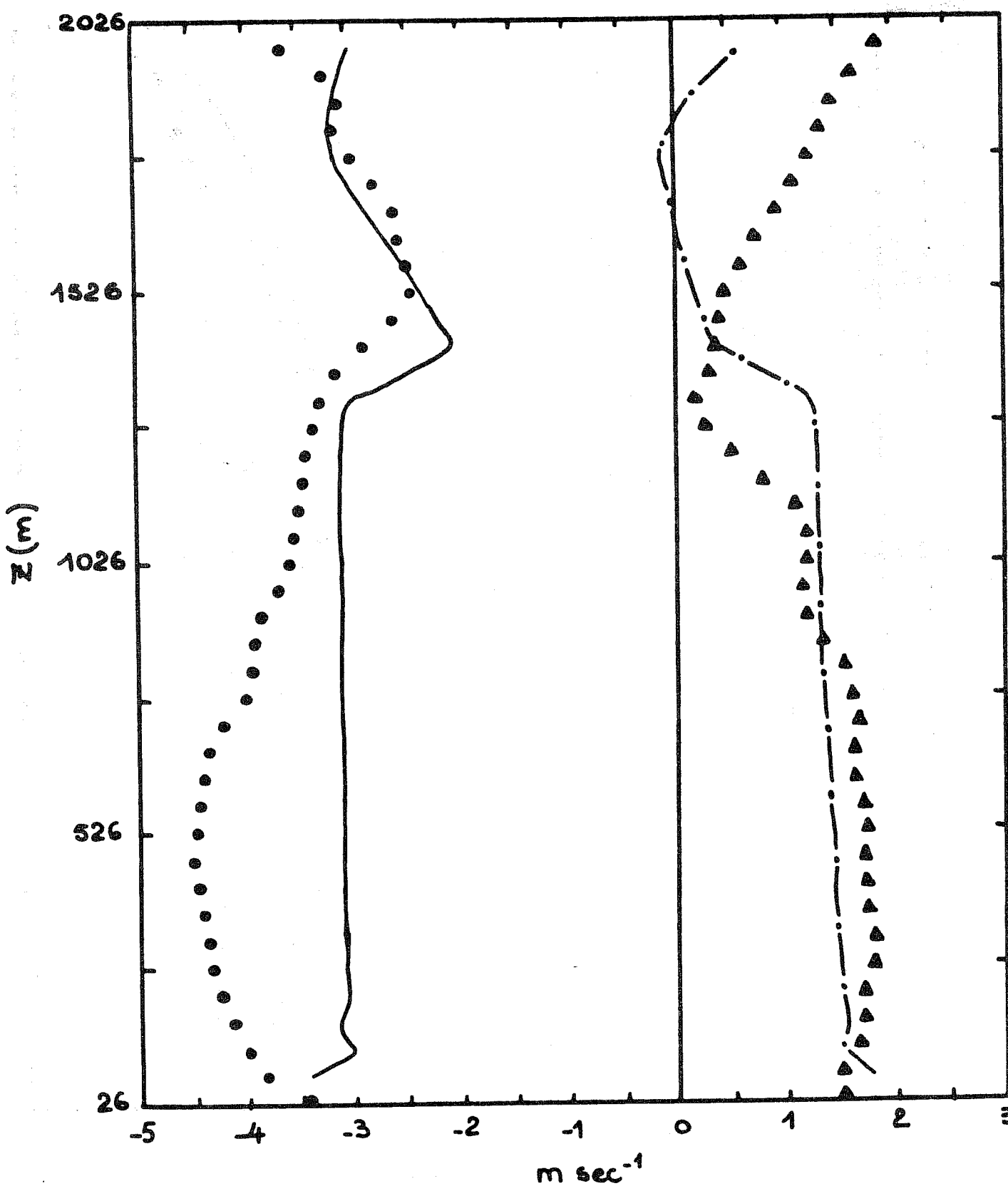

FIGURE 5d - Mean wind Profile at 16 h. ●, experimental values and _____, numerical values of the zonal wind; ▲, experimental values and -.-.-, numerical values of the meridional wind.

(ii) a rotation of the mean wind due to Coriolis effect since the $\bar{u}$-component remains almost constant (-3 msec^{-1}) while the $\bar{v}$-component evolves from -0.5 msec^{-1} at $t = 9$ h (Fig. 5a) to 0.7 msec^{-1} at $t = 12$ h (Fig. 5b), 1.0 msec^{-1} at $t = 14$ h (Fig. 5c) and 1.5 msec^{-1} at $t = 16$ h (Fig. 5d). The above features of the calculated mean wind compare favourably with those of the observed wind.

* Turbulent fluxes of heat and momentum

The turbulent heat flux $\overline{w'\theta'}(z,t)$ is shown in Fig. 6a. The evolution consists in a progressive development of a layer where the heat flux varies linearly with height according to Eq.(14) and temperature gradient evolution (Fig. 4). The negative heat flux at the top of the convective layer is related to the conversion of kinetic energy into potential energy due to the above described overshoot effect. Since turbulent heat flux was not measured during the Wangara experiment, we shall compare our results with those obtained by Deardorff (1974a) with the aid of his sophisticated subgrid-scale model (Fig. 6b): once again the agreement is very good.

Since the mean pressure gradient vanishes in the x-direction and varies linearly with height in the y-direction (Eq.(26)) and since $\bar{u}$ and $\bar{v}$ are almost constant in the convective layer (Figs. 5a to 5d), $\overline{u'w'}$ should vary linearly with height while $\overline{v'w'}$ should have a parabolic profile (Eq.(13)). These features are recovered in Figs. 7a and 7b which show the evolution of the calculated momentum flux.

* Eddy kinetic energy and temperature variance

From the preceding considerations (vanishing mean wind gradient) it results that the turbulence is generated mainly by buoyancy. In this case, Willis and Deardorff (1974) have proposed for scales for velocity and temperature in the PBL the convective velocity $w_* = (\alpha g Q_0 h)^{1/3}$ and the corresponding convective temperature $T_* = Q_0/w_*$. Consequently the vertical profile of eddy kinetic energy, made dimensionless by h and w_*^2, is shown in Fig. 8. One can notice that Willis and Deardorff's hypothesis is verified with a good accuracy and that the dimensionless eddy kinetic energy profile remains almost constant with a maximum at around $z = h/3$. The maximum value of $\bar{e}$ as well as the height at which this maximum occurs are in very good agreement with Deardorff's (1974b) results (we shall indicate for comparison that the two horizontal components of eddy kinetic energy are almost identical).

FIGURE 6a -
Heat flux profile.
-.-.-, 10 h; - - -, 11 h;
_____, 12 h; ....., 15 h.

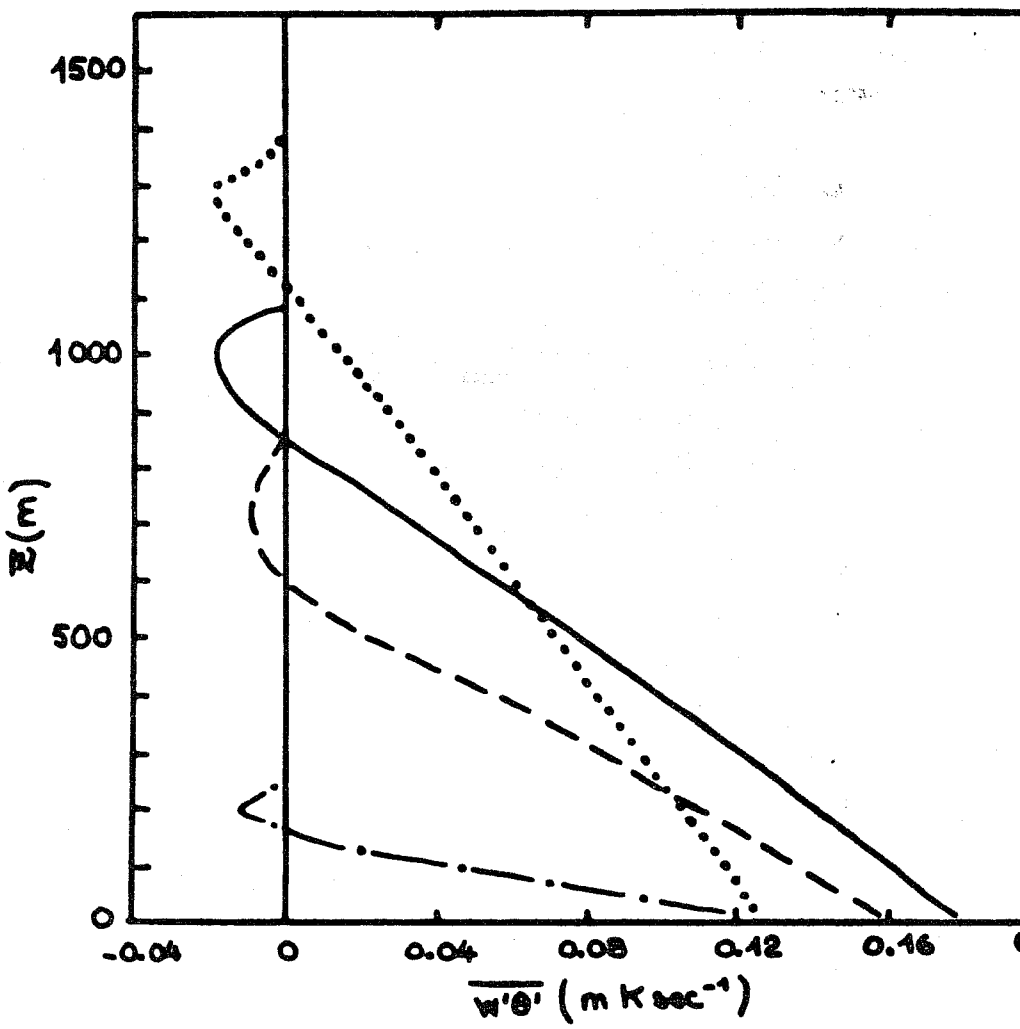

FIGURE 6b -
Heat flux profile taken
from Deardorff (1974a).
-.-.-, 10 h; - - -, 11 h;
_____, 12 h; _..._, 16 h.

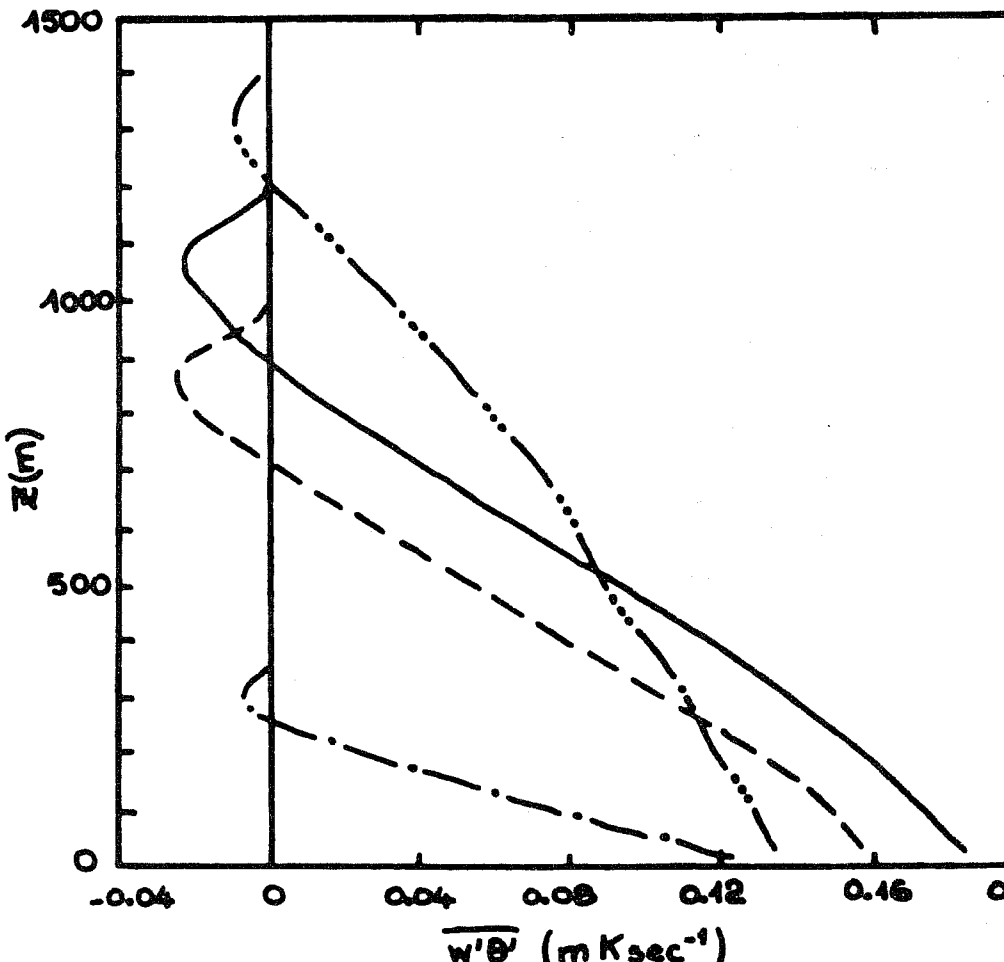

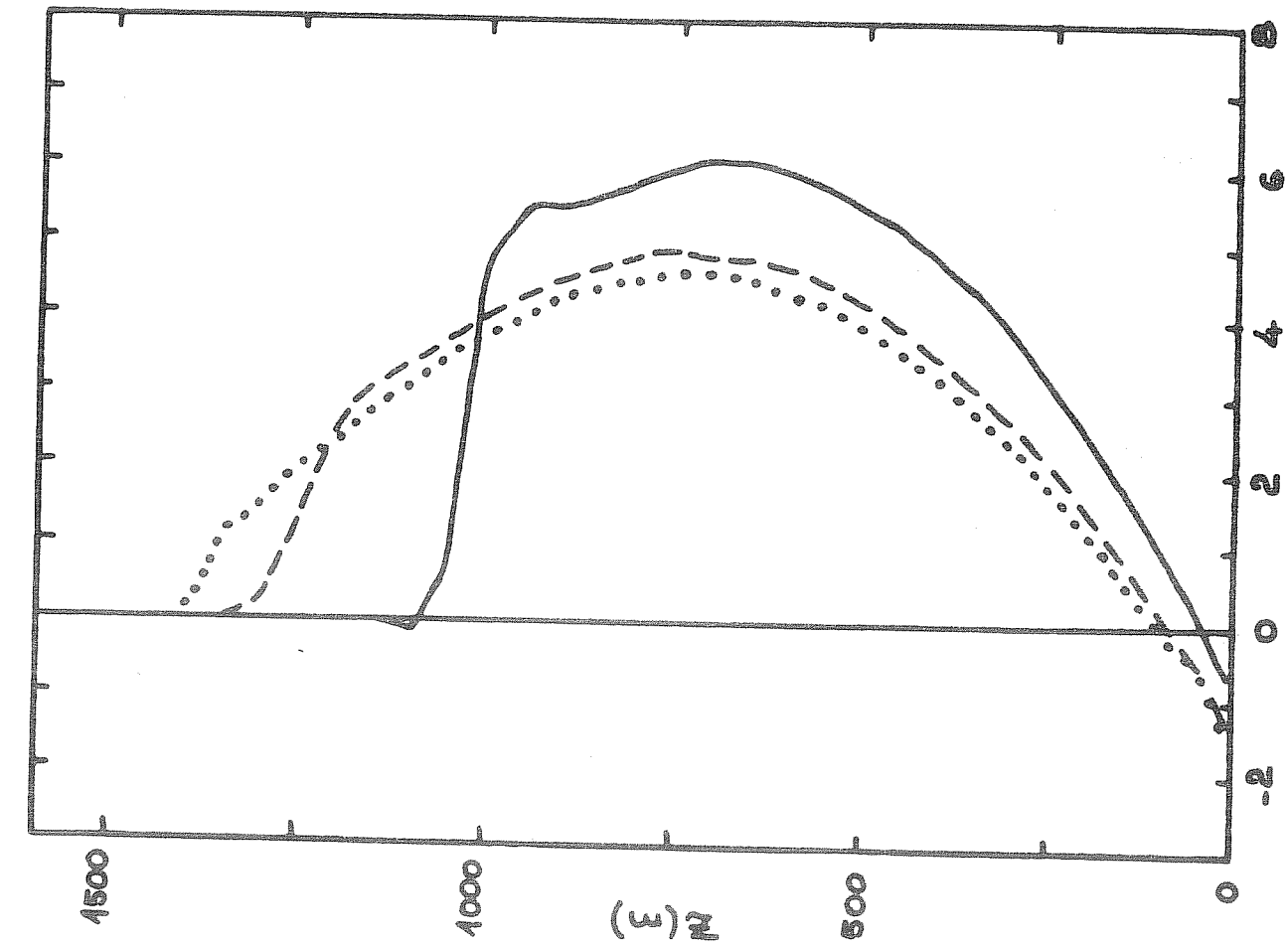

FIGURE 7b - Vertical turbulent flux of meridional wind.
——, 12 h; - - -, 14 h; ....., 16 h.

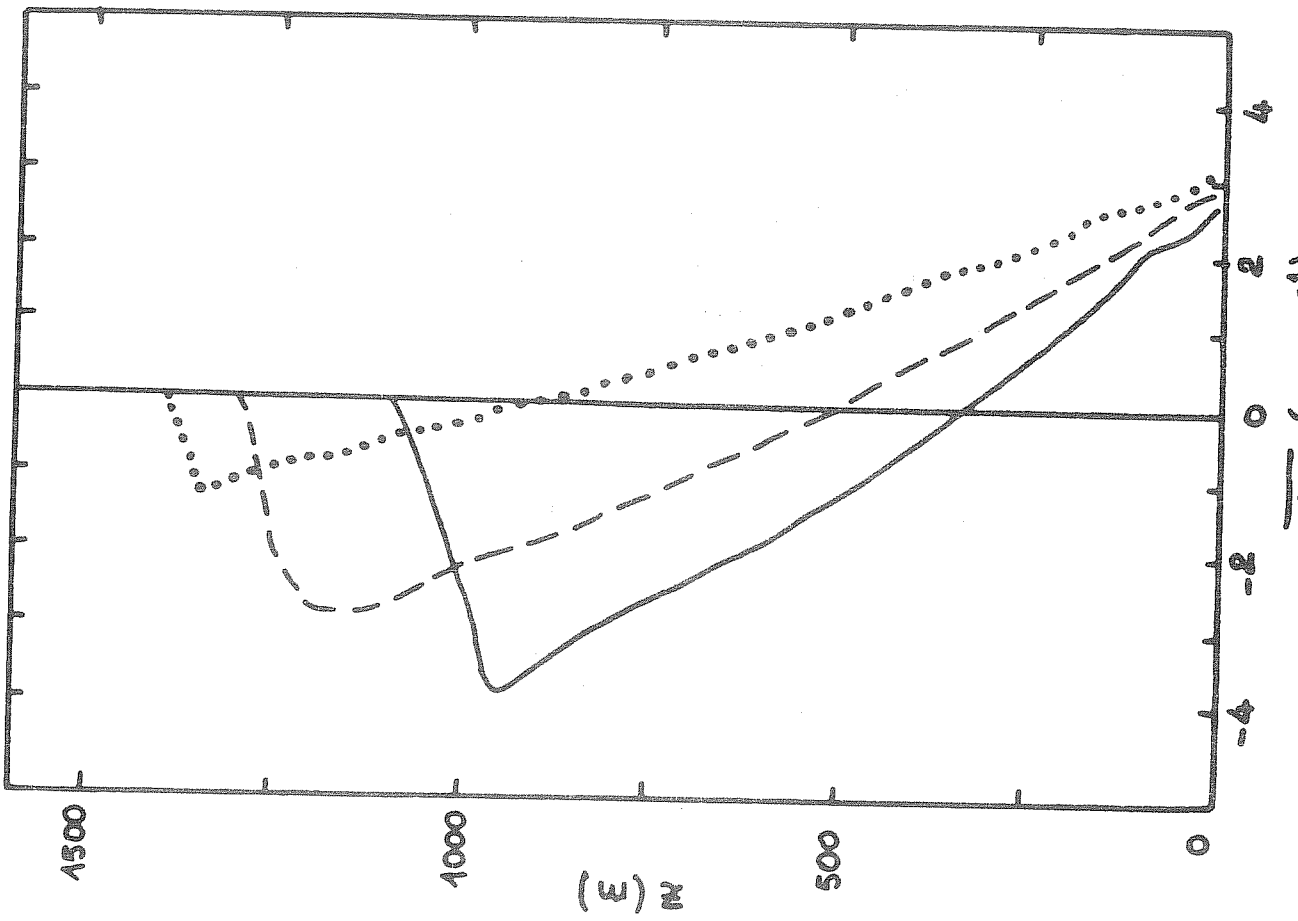

FIGURE 7a - Vertical turbulent flux of zonal wind.
——, 12 h; - - -, 14 h; ....., 16 h.

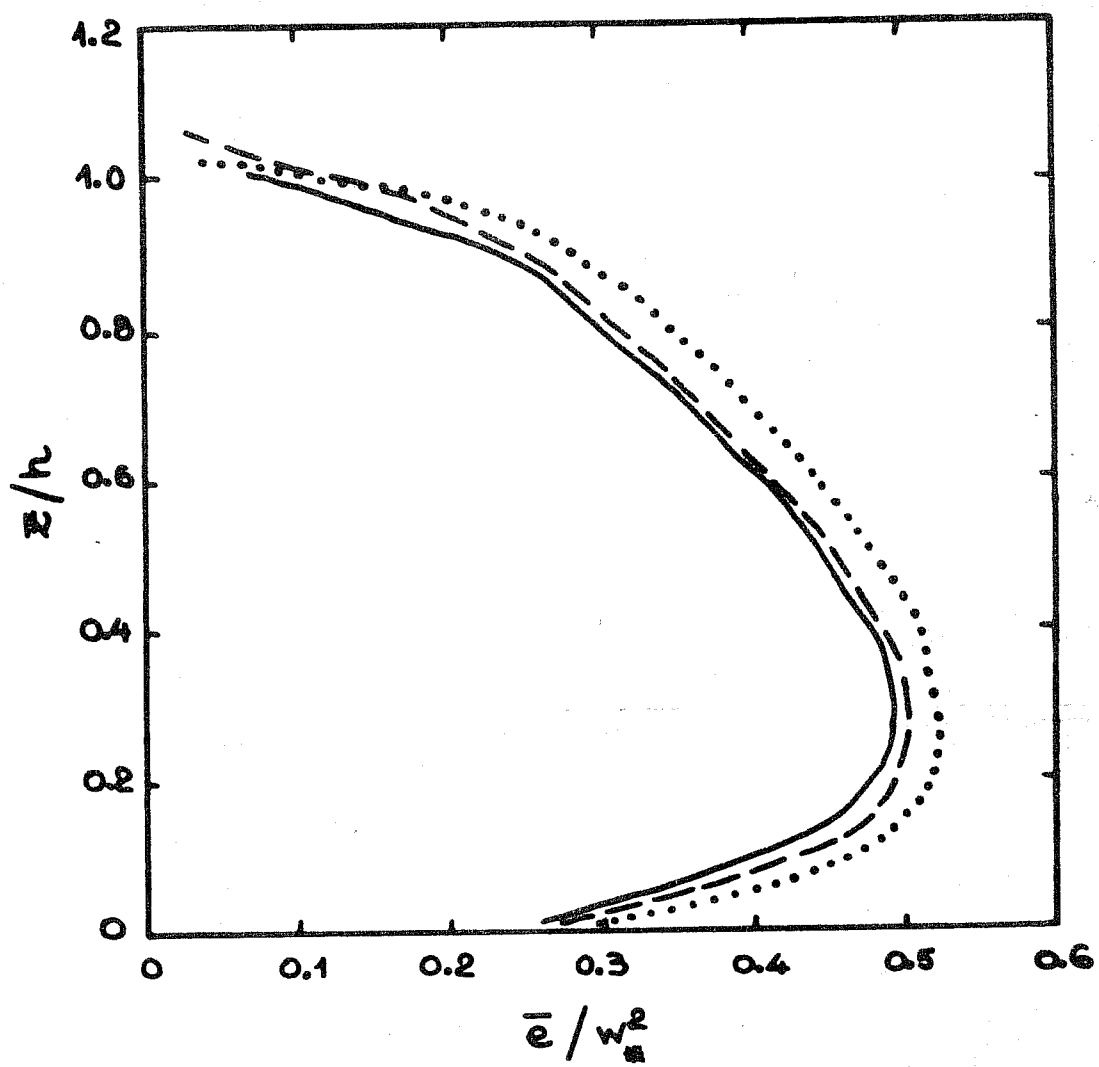

FIGURE 8 - Dimensionless eddy kinetic energy profile.
_____, 12 h; - - -, 14 h; ....., 16 h.

The eddy kinetic energy budget, represented by Eq.(15) with i=j, i.e.

$$\frac{\partial \bar{e}}{\partial t} = -\frac{\partial \overline{w'e}}{\partial z} - \overline{u'w'}\frac{\partial \bar{u}}{\partial z} - \overline{v'w'}\frac{\partial \bar{v}}{\partial z} + \alpha g\, \overline{w'\theta'} - \varepsilon \quad , \qquad (27)$$

is shown in Fig. 9a. The shear production terms are not represented since they are negligeable as compared to the other terms of the budget. It appears that eddy kinetic energy, generated essentially by buoyancy in the lower part of the PBL, is exported upwards by turbulent diffusion and converted into potential energy in the "overshoot" region. Dissipation takes place in the whole layer and its profile has the same form than the $\bar{e}$-profile, due to our choice of ε (Eq.(18)). This last remark explains that our eddy kinetic energy budget differs slightly from Deardorff's one (1974b), shown in Fig. 9b. This difficulty could be tided over by considering an equation for the rate of change of dissipation instead of our diagnostic estimation with a constant length h. We shall note that the budget is practically stationary since the numerical simulation shows that $\left| \partial \bar{e}/\partial t \right| \sim 10^{-3}\, w_*^3/h$, in good agreement with the above quoted scaling.

Dimensionless temperature variance $\overline{\theta'^2}/T_*^2$ is shown in Fig. 10. Once again the dimensionless profile is stationary in most of the PBL with two maxima corresponding to the unstable surface layer and to the inversion level, which are the only two regions where temperature gradient is significant. The fact that the scaling by T_*^2 seems not adequate around the inversion level shows that the stratification of the overlying stable layer should be taken as another parameter to determine the scaling quantities (see Willis and Deardorff, 1974). The profiles reported in Fig. 10 are in good agreement with those obtained by Deardorff (1974b).

We shall stop here the presentation of the model results but, as far as one disposes of a basis for the comparison, one can say that the structure of the other parameters is (or seems) very raisonable.

5. Possible developments and perspectives

The clipping approximation can be used to construct a model of turbulent convection in the PBL and in this case we have seen that it allows a precise description of the turbulence structure. It would be of interest to apply this model to cases where the shear driven turbulence plays a significant role: this seems possible since the clipping approximation can be used successfully for the description of laboratory channel flows (André, 1976).

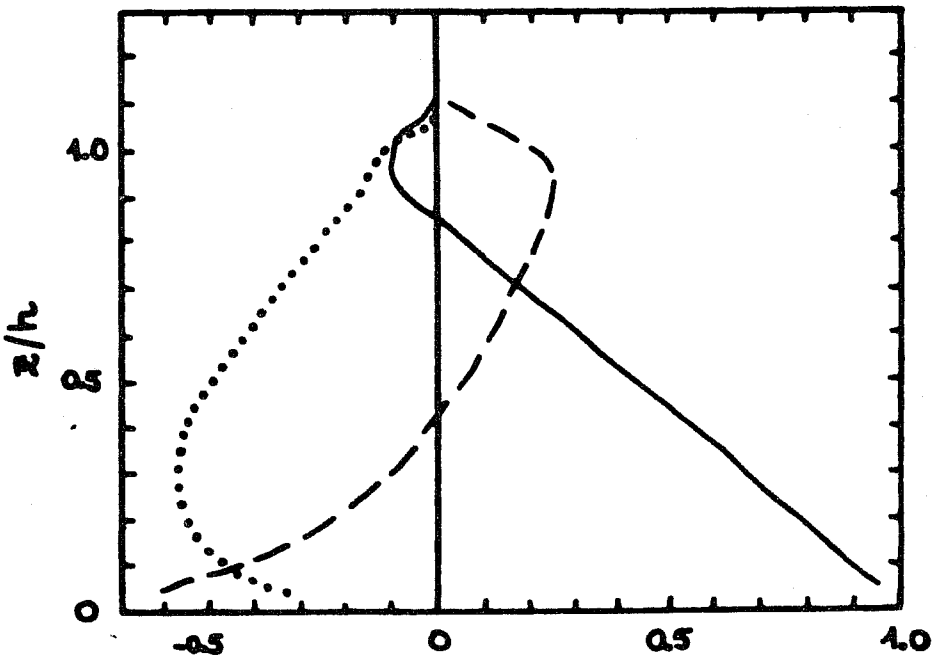

FIGURE 9a - Dimensionless eddy kinetic energy budget. _____, buoyant production; ....., dissipation; - - -, turbulent diffusion.

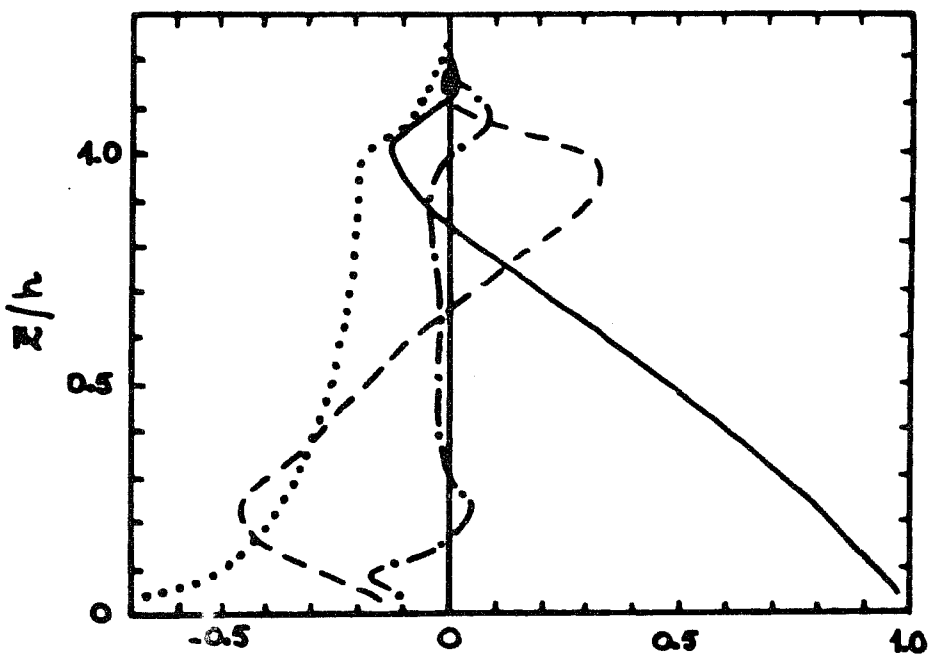

FIGURE 9b - Dimensionless eddy kinetic energy budget taken from Deardorff (1974b). _____, buoyant production; ....., dissipation; - - -, turbulent diffusion; -.-.-, pressure transport.

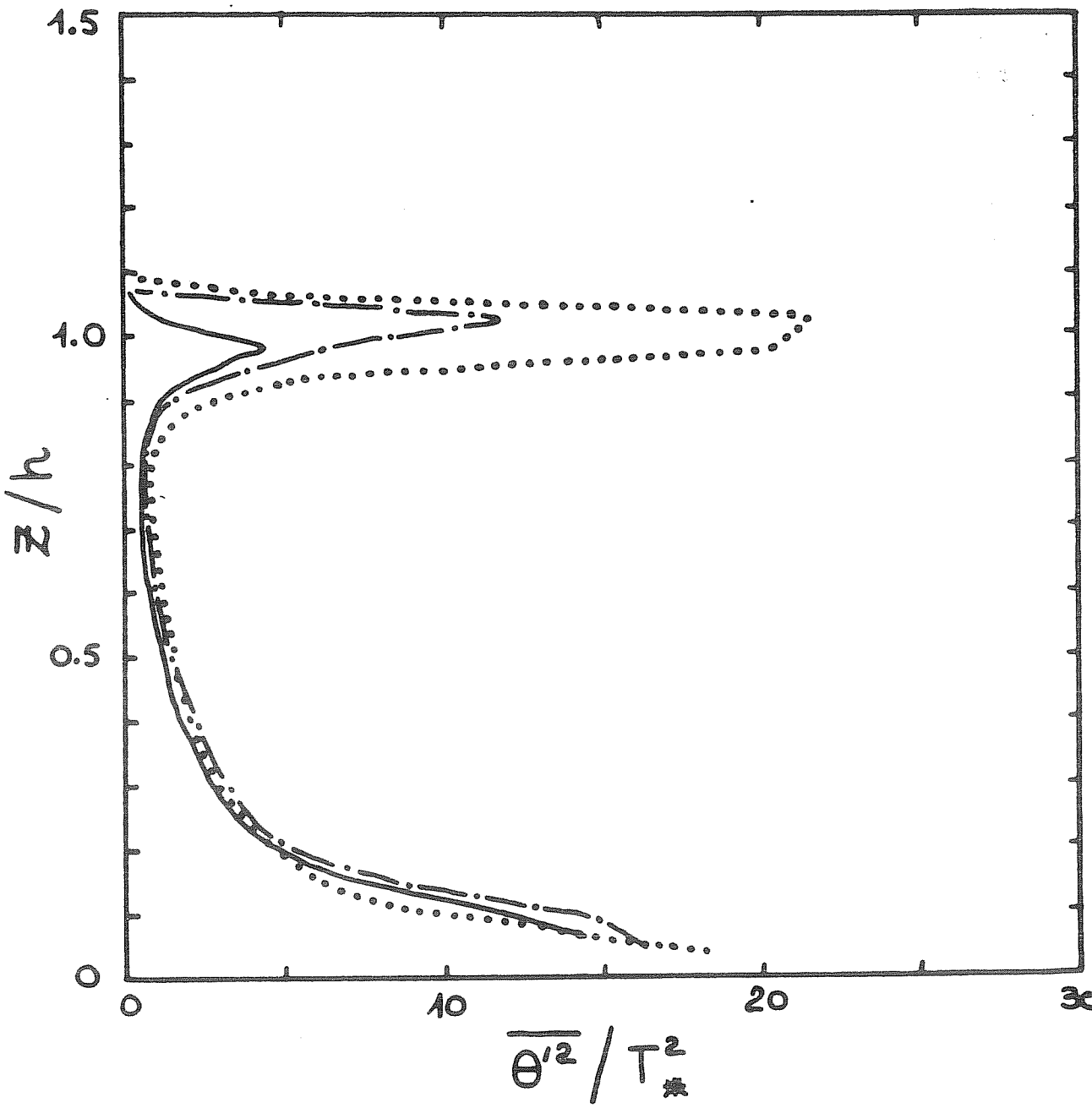

FIGURE 10 - Dimensionless temperature variance profile.
_____, 11 h; - - -, 12 h; ....., 15 h.

Another interesting development of the model would consist in including water vapor and radiative transfer; this would give the possibility to describe the behavior of nocturnal PBL since it is known that in this case turbulence and radiative transfer have almost the same importance with respect to temperature evolution (see e.g. Coantic 1975). A second step in the development of the model could consist in including the parametrization of condensation and evaporation in order to allow for the description of cloudy PBL. Unfortunately the horizontal homogeneity assumption, which is necessary if one wants to avoid the complexity of three-dimensional modelling, will probably restrict the application of the model to PBL with stratified clouds but this represents anyway a significant percentage of PBL situations.

At any stage of its development the model can be considered as a "numerical laboratory" which can be used to:
(i) study some particular cases of PBL evolution when one does not dispose of the corresponding experimental studies;
(ii) test the accuracy of various PBL parametrizations (particularly those which are included in numerical wheather forecasting schemes).
In this respect the small computing time required by the model (100 sec of CDC 6600 computing time for a one hour simulation for the case described in section 4) is a very favourable characteristic which allows numerous numerical case studies.

I would like to thank B.E. Launder for valuable suggestions in the field of parametrization of pressure effect on triple correlation evolution. Thanks are also due to P. Fouques Duparc for his participation to the numerical experiments.

References

André, J.C., 1976: Thesis, University of Paris 6.

André, J.C., G. De Moor, P. Lacarrère & R. du Vachat, 1976a: J. Atmos. Sci., 33, 476-481.

_____, 1976b: J. Atmos. Sci., 33, 482-491.

Blanchet, J., 1970: La Météorologie V, 15, 15-78.

Clarke, R.H., 1974: Izv. Atmos. Oceanic Phys., 10, 360-374.

Clarke, R.H., A.J. Dyer, R.R. Brook, D.G. Reid & A.J. Troup, 1971: Paper N°19 Div. Meteor. Phys., CSIRO, Australia.

Coantic, M., 1975: Course AMES 222C, University of California, San Diego.

Daly, B.J., & F.H. Harlow, 1970: Phys. Fluids, 13, 2634-2649.

Deardorff, J.W., 1966: J. Atmos. Sci., 23, 503-506.

_____, 1972: J. Atmos. Sci., 29, 91-115.

_____, 1973: J. Fluids Eng., 95, 429-438.

_____, 1974a: Boundary-Layer Meteor., 7, 81-106.

_____, 1974b: Boundary-Layer Meteor., 7, 199-226.

Donaldson, C.duP., 1973: In "Workshop on Micrometeorology", Boston, Amer. Meteor. Soc., 313-392.

Launder, B.E., 1975: J. Fluid Mech., 67, 569-581.

Launder, B.E., G.J. Reece & W. Rodi, 1975: J. Fluid Mech., 68, 537-566.

Lewellen, W.S., & M. Teske, 1973: J. Atmos. Sci., 30, 1340-1345.

Lumley, J.L., & B. Khajeh-Nouri, 1974: Adv. Geophys., 18A, 169-192.

Millionshchikov, M., 1941: C.R. Acad. Sci. URSS, 32, 615-618.

Monin, A.S., & A.M. Obukhov, 1954: Tr. Geofiz. Inst. Akad. Nauk SSSR, 151, 163-187.

Monin, A.S., & A.M. Yaglom, 1971: "Statistical Fluid Mechanics: Mechanics of Turbulence", Cambridge, M.I.T. Press.

O'Brien, E.E., & G.C. Francis, 1962: J. Fluid Mech., 13, 369-375.

Ogura, Y., 1963: J. Fluid Mech., 16, 33-40.

Orszag, S.A., 1970: J. Fluid Mech., 41, 363-386.

Paulson, C.A., 1970: J. Appl. Meteor., 9, 857-861.

Prandtl, L., 1925: Z. Angew. Math. Mech., 5, 136-139.

Smagorinsky, J., 1963: Mon. Wea. Rev., 91, 99-164.

Somméria, G., 1974: Thesis, University of Paris 6.

_____, 1976: J. Atmos. Sci., 33, 216-241.

Turner, J.S., 1973: "Buoyancy Effects in Fluids", Cambridge, Cambridge University Press.

du Vachat, R., 1976: Realizability inequalities in turbulent flows, to be published.

Willis, G.E., & J.W. Deardorff, 1974: J. Atmos. Sci., 31, 1297-1307.

Wyngaard, J.C., 1973: In "Workshop on Micrometeorology", Boston, Amer. Meteor. Soc., 101-149.

Wyngaard, J.C., & O.R. Coté, 1974: Boundary-Layer Meteor., 7, 289-308.

Wyngaard, J.C., O.R. Coté & K.S. Rao, 1974: Adv. Geophys., 18A, 193-211.

Yamada, T., & G. Mellor, 1975: J. Atmos. Sci., 32, 2309-2329.